Progress In Electromagnetics Research C, Vol. 119, 145–159, 2022

A Compact Microstrip Four Port Dual Circularly Polarized MIMO Antenna for Sub-6G Application

Zhong Yu[1], Leiyan Huang[1, *], Qi Gao[1], and Yanping Chen[2]

Abstract—This article proposes a compact microstrip four-port dual circularly polarized (CP) multiple-input multiple-output (MIMO) antenna with polarization diversity for Sub-6G band. The proposed MIMO antenna consists of four antenna elements, two of which are left-hand circular polarization (LHCP), and the other two are right-hand circular polarization (RHCP). The circular polarization of each antenna element of the MIMO antenna is achieved by a microstrip feed line and a slotted ground plane with two rectangular strips. A novel decoupling element of the antenna composed of I-shaped and II-shaped metal strips is cross-connected and merged between the ground planes of the antenna to obtain wide axial ratio bandwidth and high isolation. The size of the proposed antenna is $55 \times 55 \times 1.6\,\text{mm}^3$. The antenna of the impedance bandwidth ($S_{11} \leq -10\,\text{dB}$) is 3.28–3.80 GHz (14.6%), and the axial ratio bandwidth (AR $\leq 3\,\text{dB}$) is 2.85–3.87 GHz (30.3%). Inter-element isolation less than $-16\,\text{dB}$ and the envelope correlation coefficient (ECC) less than 0.07 are achieved between the ports of the antenna. The proposed MIMO antenna achieves full coverage of CP characteristics within the impedance bandwidth. The proposed antenna is beneficial to the application of Sub-6G band. At the same time, it is also suitable for dual circular polarization communication and polarization diversity system.

1. INTRODUCTION

Circularly polarized (CP) antennas have special advantages in radio wave propagation. For example, the transmitting or receiving of signals does not depend on the direction of the antenna orientation, CP antennas immunity toward polarization mismatch, and multipath distortion effect [1]. Furthermore, CP antennas are able to reduce Faraday rotation effect occurring in the ionospheric layer of the atmosphere [2, 3]. These advantages of circular polarization make them potentially valuable in multiple-input multiple-output (MIMO) wireless systems. Microstrip CP MIMO antennas achieve high-quality wireless communication systems because of their outstanding characteristics in terms of expanding channel capacity, improving spectrum efficiency, and reducing production costs [4].

In the past ten years, several researchers have proposed some CP MIMO antennas for WLAN, C-band, and satellite applications [5–8]. A planar two-port CP MIMO antenna is composed of two physically separated upper and lower radiators [5]. The CP performance is in the $5.8 \sim 6.0\,\text{GHz}$ frequency band, and the isolation is $-15\,\text{dB}$. The axial ratio bandwidth (ARBW) range of the planar three-element MIMO antenna is $5.61 \sim 5.70\,\text{GHz}$, and the offset feeding is used for achieving right-hand circular polarization (RHCP) and enhancing the ARBW [6]. The designed antenna has left-hand circular polarization (LHCP) characteristics at 30 GHz. The coupling suppression behavior of frequency selective surface (FSS) in CP MIMO antenna system is studied in [7]. The presented antenna has the total geometry of $165 \times 165\,\text{mm}^2$ which accomplishes 201 MHz ARBW at WLAN band [8]. Among

Received 6 February 2022, Accepted 4 March 2022, Scheduled 29 March 2022

* Corresponding author: Leiyan Huang (hly814@stu.xupt.edu.cn).

[1] School of Communication and Information Engineering, Xi'an University of Posts & Telecommunications, Xi'an, China. [2] School of Computer Science & Technology, Xi'an University of Posts & Telecommunications, Xi'an, China.

these CP MIMO antennas reported above, the CP waveform generated by the antenna is single, which generates LHCP or RHCP waves. Simultaneously generating two CP waves in a single antenna can significantly improve antenna performance. It is necessary to research on dual circularly polarized MIMO antennas.

Dual-CP antenna applies the polarization diversity principle. Polarization diversity reduces the coupling between antenna elements without increasing the antenna size and improves antenna performance by increasing diversity gain and channel capacity [9, 10]. The ability of dual-CP MIMO antennas to achieve frequency reuse, increase channel capacity, reduce mutual coupling, and reduce multipath fading effects has attracted the attention of researchers [11, 12].

In recent years, the MIMO antennas that can generate dual-CP waves at the same frequency have become the need of today's wireless world [13–16]. Two asymmetric T-shaped feeders are placed in orthogonal directions to generate two orthogonal electric fields to achieve dual circular polarization, and the 3-dB AR bandwidth of the antenna is about 59.65% (2–3.7 GHz) [13]. The antenna is fed by two coplanar waveguides (CPWs), which can generate dual circularly polarized waves [14]. The dual-port CP MIMO antenna implements RHCP and LHCP by extending the right ground plane and left ground plane of the CPW in the y direction to improve link reliability, AR $\leq$ 3 dB from 5.2 GHz to 6.3 GHz with 100% bandwidth overlap between the impedance and axial ratio bandwidths [15]. A planar and compact circularly polarized MIMO patch antenna with polarization diversity is presented [16]. Three grounded stubs and a mirrored F-shaped defected ground structure are used to achieve simultaneous matching and isolation between the two patches with offset feeding for circular polarization. In addition, the importance of a common ground plane of MIMO antennas is discussed [17]. The same reference voltage level for MIMO antennas is achieved by having a common ground plane. Therefore, the ground plane of the antenna radiator is not connected and might not be used in practical applications [8].

This paper presents a compact microstrip four-port dual CP MIMO antenna that works in the 3.5G frequency band. The antenna consists of four dual-CP antenna elements and a novel decoupling element structure. The isolation and ARBW of the antenna are improved through polarization diversity as well as the decoupling element. The proposed antenna achieves dual-CP characteristics in Sub-6G band. In the second part, the analysis process and simulation results of the proposed dual-CP antenna element and dual-CP MIMO antenna structure are given. The third part provides measurement results to verify the performance of the proposed antenna system. Finally, the fourth part provides conclusions.

2. ANTENNA CONFIGURATION

2.1. Proposed Circularly-Polarized Antenna Element Design

Figure 1 shows the structure of the CP antenna element, used as a radiating element of the proposed MIMO antenna. The dimensions of the antenna element are given in Table 1. The antenna element is designed on an FR-4 substrate (with relative permittivity of 4.4 and loss tangent of 0.02) of size $25 \times 25 \times 1.6\,\text{mm}^3$. The antenna element is excited using a microstrip feed line of 50 Ω. A 3-D electromagnetic simulation software (ANSYS HFSS) is used for antenna design.

Table 1. The dimensions of the antenna element/MIMO antenna.

Parameter	Value (mm)	Parameter	Value (mm)
L_1	25	w_f	3
W_1	25	h	1.6
l_1	21	L_2	55
l_2	3	W_2	55
w_1	8	l_3	7
w_2	7	l_4	5
w_3	3	l_5	0.5
l_f	12	w_4	20.25

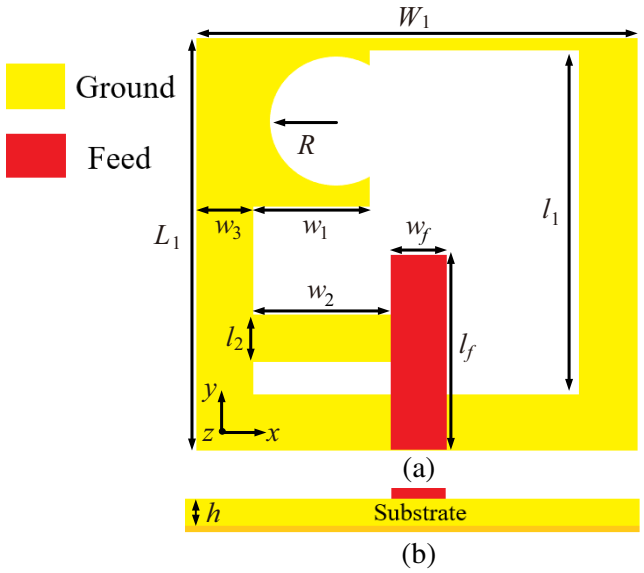

Figure 1. Structure layout of the proposed antenna element: (a) top view; (b) side view.

2.1.1. Design Process

The design procedure of the proposed antenna element structure, which is used as an element of the presented MIMO antenna, is presented in Figure 2. In Figure 2(a), the antenna of step-1 has a basic

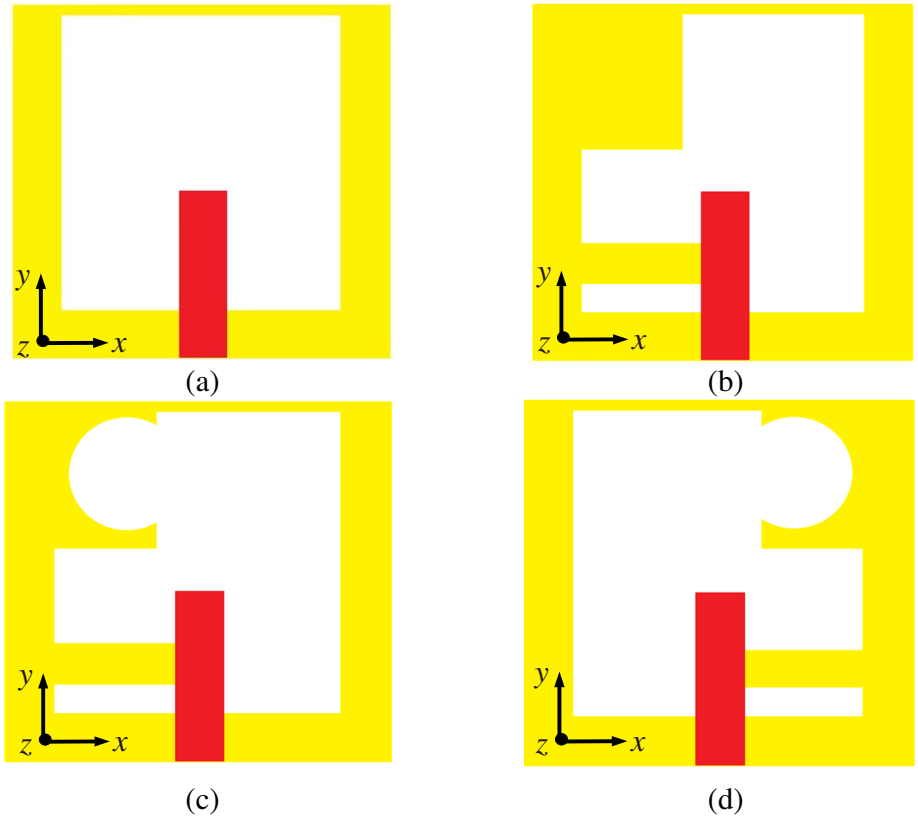

Figure 2. Evolution steps of the antenna element: (a) step-1; (b) step-2; (c) step-3 (proposed antenna element); (d) step-4 (mirror image of the proposed antenna element).

square slot, and feed structure has used a microstrip feedline [9]. The size change of the square slot optimizes the current path or resonant frequency band of the antenna. In Figure 2(b), CP radiation is achieved by merging two rectangular bars in the upper left and lower left corners of the ground. The rectangular strips establish a phase difference of 90° between E_{xoy} and E_{yoz} to achieve CP radiation, which also causes the resonant frequency of the antenna to shift to high frequencies. Therefore, the antenna structure needs further optimization to ensure excellent antenna performance. A semi-circular slot is etched on the rectangular strip in the upper left corner, as shown in Figure 2(c). The new semi-circular slot structure allows the antenna element performance to be further optimized. Among them, the resonant frequency and axial ratio frequency of the antenna are both shifted to low frequency. In Figure 2(d), a mirrored shape of the designed antenna element is illustrated, which is the mirror image of the antenna element (shown in Figure 1).

2.1.2. Antenna Analysis

The reflection coefficient (S_{11}) and axial ratio of the antenna element for each step are given in Figures 3(a), (b). The proposed antenna element resonates at 2.86–4.09 GHz frequency band with 3-dB ARBW of around 324 MHz (3.255–3.577 GHz). Obviously, the low-frequency operating frequency of the antenna element is achieved by etching the semi-circular slot in the rectangular strip. Among them, the resonant frequency is shifted by 220M to the low frequency, and the axial ratio frequency is shifted by 170M to the low frequency. In addition, Figures 3(a), (b) show that the S_{11} and ARBW of the antenna element is at the same frequency band as the mirror antenna. This feature is rare in the dual-CP antennas currently designed.

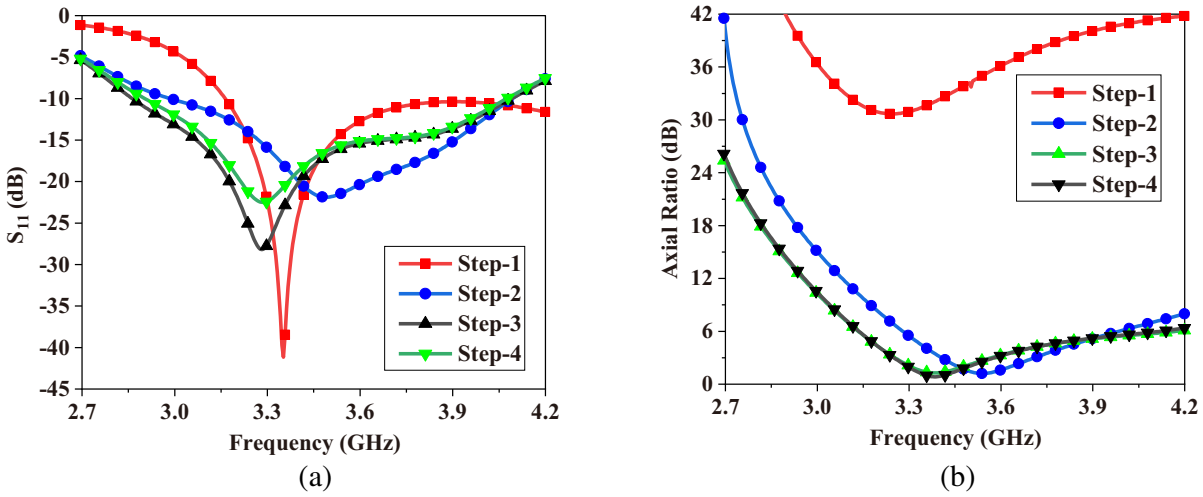

Figure 3. Comparison of the antenna element design steps: (a) reflection coefficient; (b) axial ratio.

2.1.3. Dual-Circular Polarization Mechanism

The surface current distributions of the proposed antenna element and its mirror image are studied to explain the dual-CP mechanism. Figures 4 and 5 show the surface current distributions of the two antennas at 3.4 GHz (for 0°, 90°, 180° and 270° phases, respectively). The current distribution changes as the feeding phase changes from 0° to 270°.

The dominant current vectors in Figure 4 rotates counterclockwise, which illustrates the RHCP operation of the antenna element. Furthermore, in Figure 5, the dominant current vector in antenna element mirror image rotates clockwise, hence validating the LHCP operation.

It can be further illustrated from the radiation patterns of Figures 6(a), (b) that the proposed antenna element radiates RHCP waves in $+z$ direction while its mirror image radiates LHCP waves in $+z$ direction.

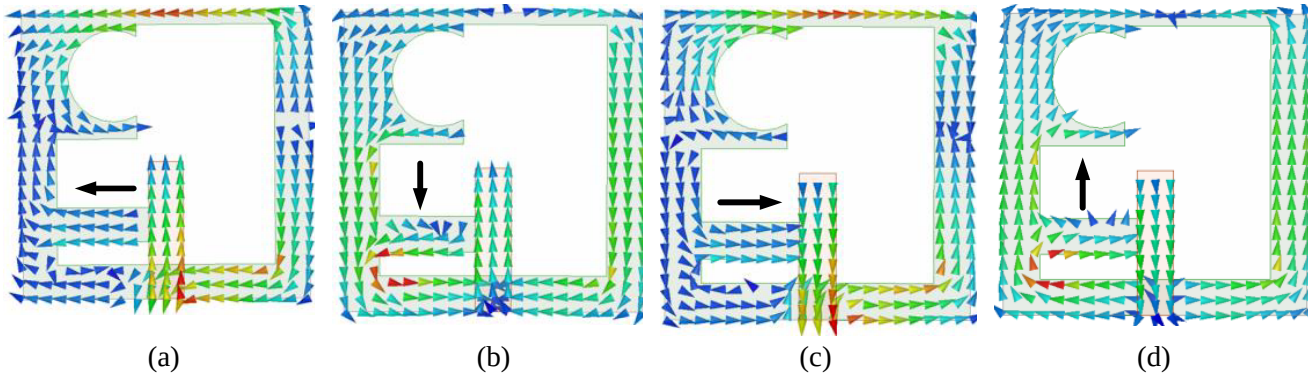

Figure 4. Surface current distributions in the proposed antenna element at 3.4 GHz: (a) $\omega t = 0°$; (b) $\omega t = 90°$; (c) $\omega t = 180°$; (d) $\omega t = 270°$.

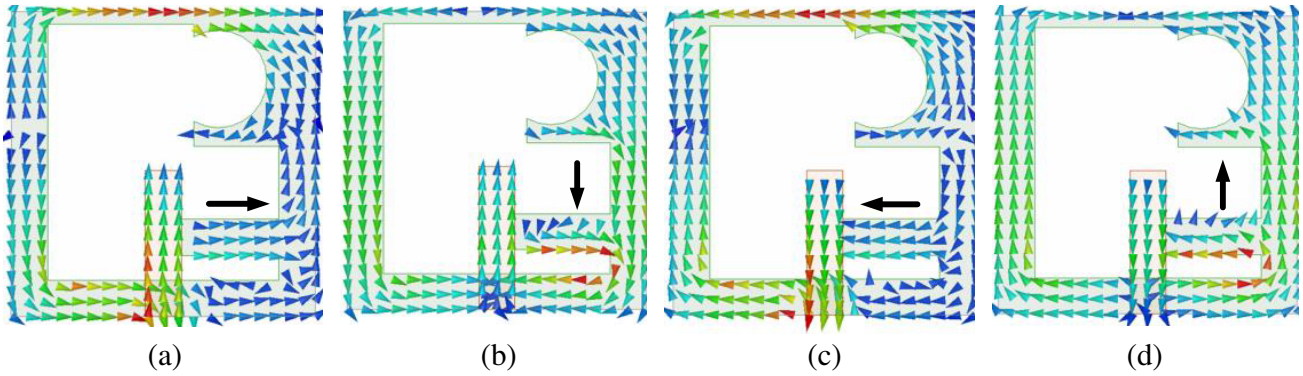

Figure 5. Surface current distributions in the mirror image of proposed antenna element at 3.4 GHz: (a) $\omega t = 0°$; (b) $\omega t = 90°$; (c) $\omega t = 180°$; (d) $\omega t = 270°$.

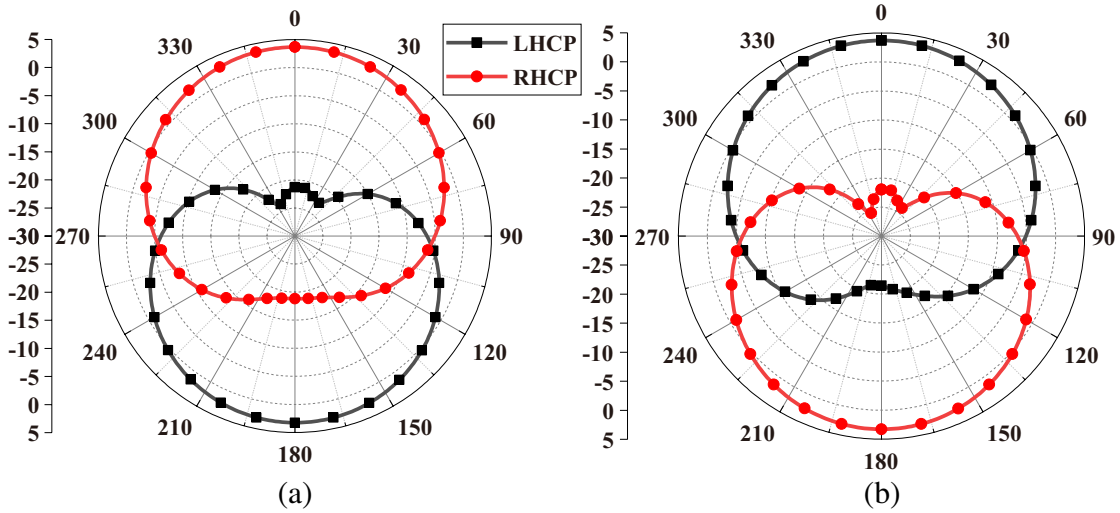

Figure 6. Simulated radiation patterns at 3.4 GHz: (a) proposed antenna element, (b) mirror image of the proposed antenna element.

2.2. Proposed Four-Port Dual Circularly Polarized Multiple-Input-Multiple-Output (CP MIMO) Antenna

The dual-CP MIMO antenna configurations designed with the help of the proposed antenna element and its mirror image are shown in Figure 7. The four-antenna elements are positioned at the corners of the square-shaped substrate. The inter-element spacing is $0.057\lambda_0$ (for $f_c = 3.45\,\text{GHz}$) between MIMO radiating elements to maintain the 3-dB ARBW of the antenna element. The antenna radiates LHCP waves when elements 1 and 4 are excited, and RHCP waves when elements 2 and 3 are excited.

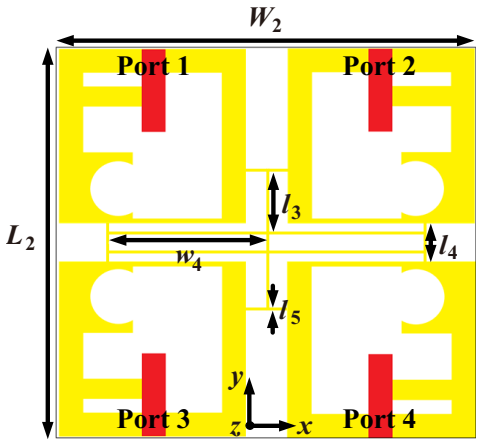

Figure 7. Structure layout of the proposed dual-CP MIMO antenna.

A decoupling element is added in the designed MIMO antenna. The decoupling element is composed of I-shaped strip and II-shaped strip cross-connected with the ground plane of the MIMO antenna to achieve the purpose of increasing the isolation between internal components and restoring the CP performance. The design parameters are shown in Table 1.

2.2.1. Antenna Analysis

The interference of adjacent antenna elements in the dual-CP MIMO antenna will deteriorate the axial ratio. Retaining CP characteristics of the antenna elements is quite challenging in ground-connected CP MIMO antenna.

The reduction of coupling between antenna elements and the recovery of CP characteristics of the antenna are realized by the distance between antenna elements, polarization diversity, and decoupling elements. The elements in the mentioned MIMO antenna are arranged in a mirror image form, while maintaining the impedance bandwidth of the antenna at appropriate intervals and reducing the mutual influence between the antenna elements. The compact geometry of the dual-CP MIMO antenna is obtained by optimizing the spacing and position of the decoupling elements. The above method cannot significantly improve the isolation of the antenna, and introducing a decoupling element between the antenna elements is a key technology of this antenna design.

Figure 7 shows that the decoupling element is an orthogonal connection of I-shaped and II-shaped metal strips. The decoupling element realizes the circular polarization characteristics of the MIMO antenna by changing the current direction of each antenna element at different phases. The optimized decoupling element not only improves the isolation performance and restores the circular polarization characteristics, but also connects the ground plane between the antenna elements to ensure the practicability of the proposed antenna. Figures 8(a), (b) show the comparison of S_{11}, S_{21} and axial ratio changes of the MIMO antenna with or without decoupling element. The coupling of various radiation sources makes the antenna unable to achieve CP characteristics. The decoupling element improves the isolation ($S_{21} < -15\,\text{dB}$), restores the CP characteristics, and achieves the complete coverage of CP characteristics in the operating frequency range.

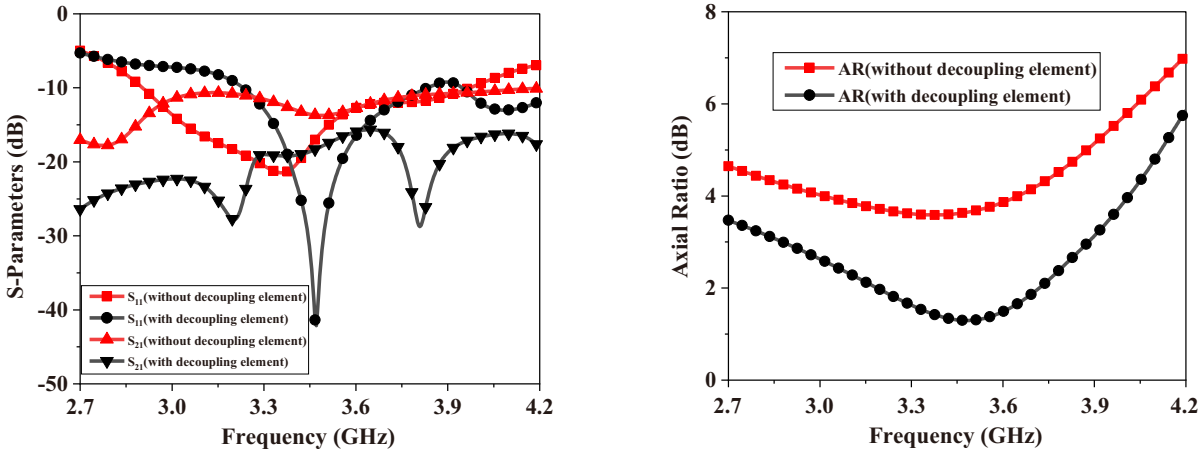

Figure 8. Effect of decoupling element on MIMO antenna performance: (a) *S*-parameters; (b) axial ratio.

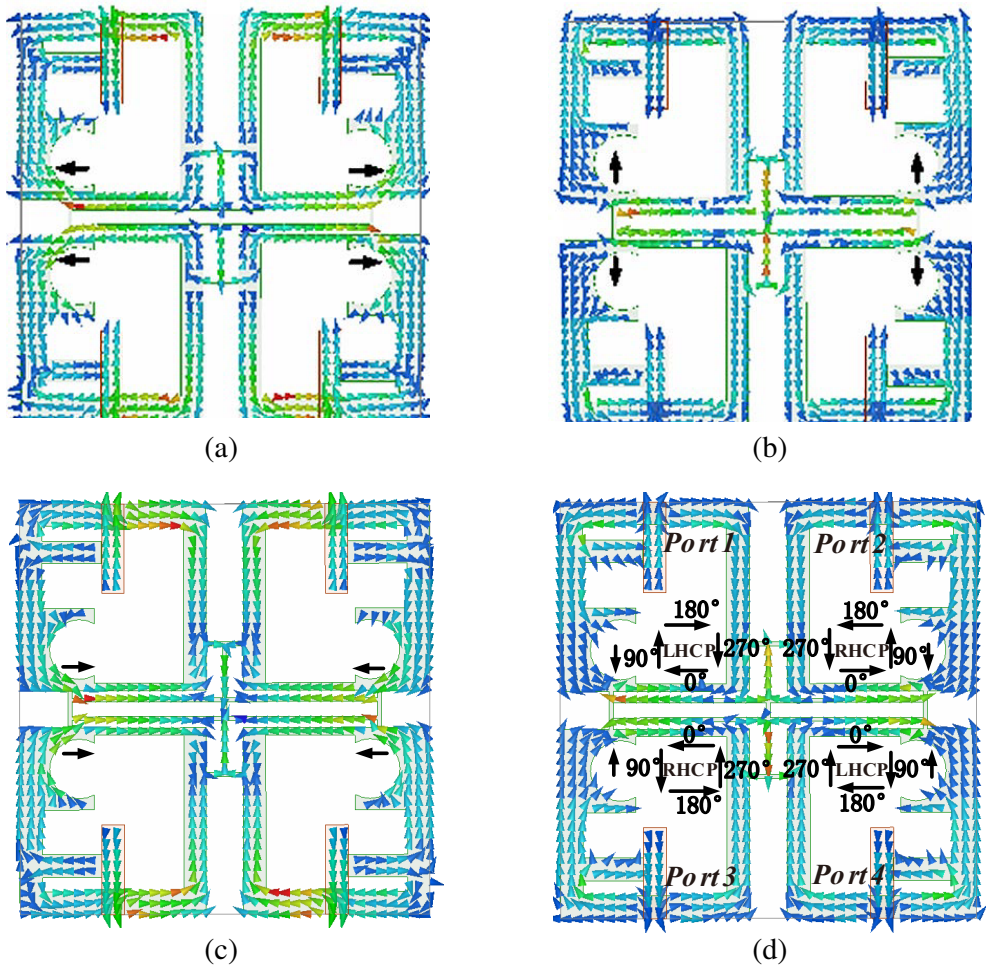

Figure 9. Surface current distributions in the dual-CP MIMO antenna at 3.45 GHz: (a) $\omega t = 0°$; (b) $\omega t = 90°$; (c) $\omega t = 180°$; (d) $\omega t = 270°$.

2.2.2. Dual-Circular Polarization Mechanism

The dual-CP characteristic of the proposed MIMO antenna is analyzed by surface current distribution. Figures 9(a)–(d) show the surface current distribution of the antenna at 3.45 GHz (for different phases) when four ports are excited at the same time, which further illustrates the dual-circular polarization mechanism of the antenna.

The direction of the main current vector at each port of the mentioned antenna changes at different phases. At 0° and 180° phases, the current distributions of port 1 and port 2 are equal and opposite in phase. At phase 90°, the main current vectors of the two ports (port 1 and port 2) are in the $+y$ direction. At phase 270°, the main current vectors of the two ports (port 1 and port 2) are in the $-y$ direction. Similarly, at 0° and 180° phases, the current distributions of port 3 and port 4 are equal and opposite in phase. At phase 90°, the main current vectors of the two ports (port 3 and port 4) are in the $-y$ direction. At phase 270°, the main current vectors of the two ports (port 3 and port 4) are in the $+y$ direction. Therefore, as shown in Figure 9(d), the current vectors at port 1 and port 4 rotate in the clockwise direction, showing the LHCP operation of antenna elements 1 and 4. The current vectors at port 1 and port 4 rotate in the counterclockwise direction, showing the RHCP operation of antenna elements 2 and 3.

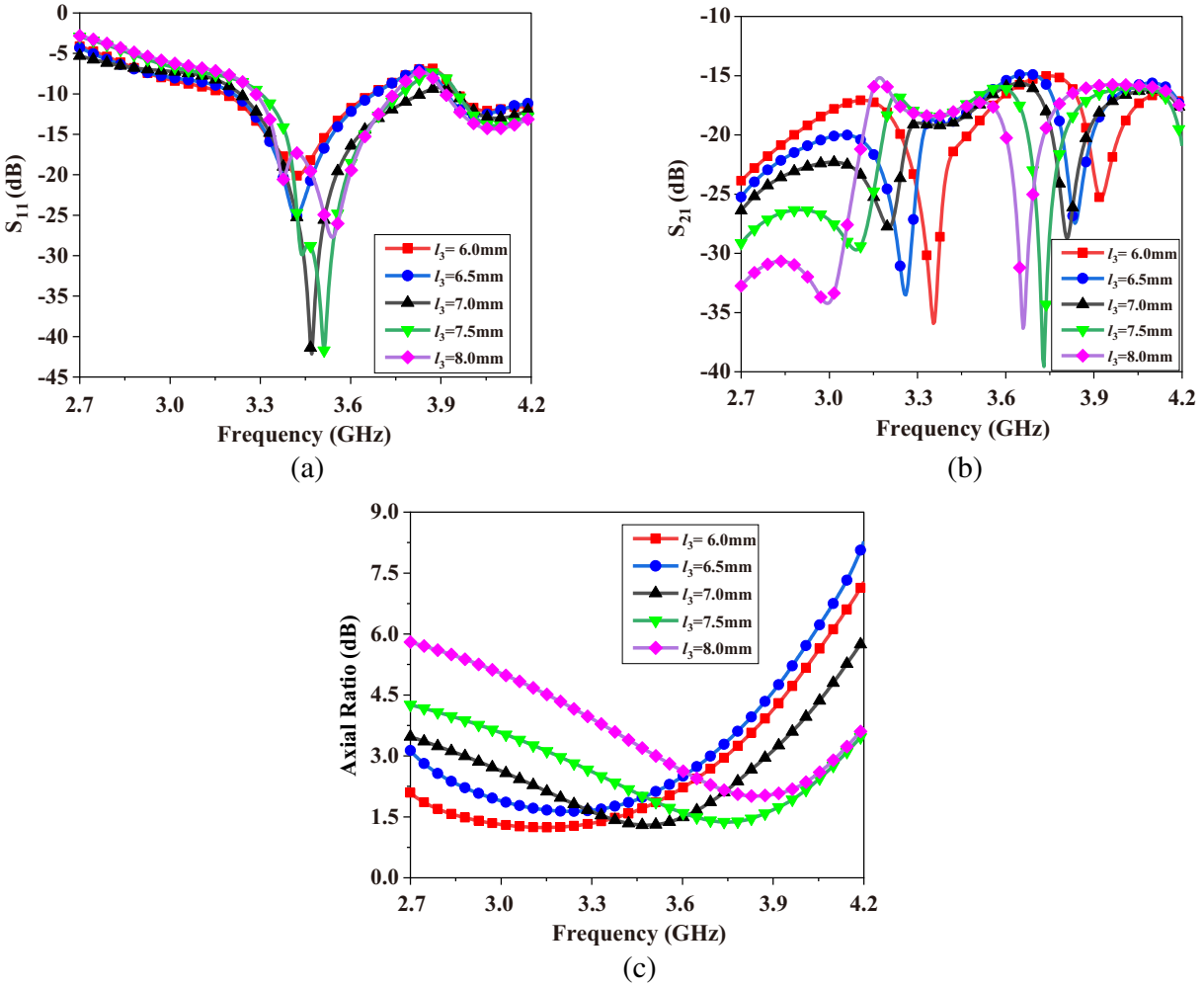

Figure 10. Variation of: (a) S_{11}; (b) S_{21}; (c) axial ratio l_3 with different length l_3.

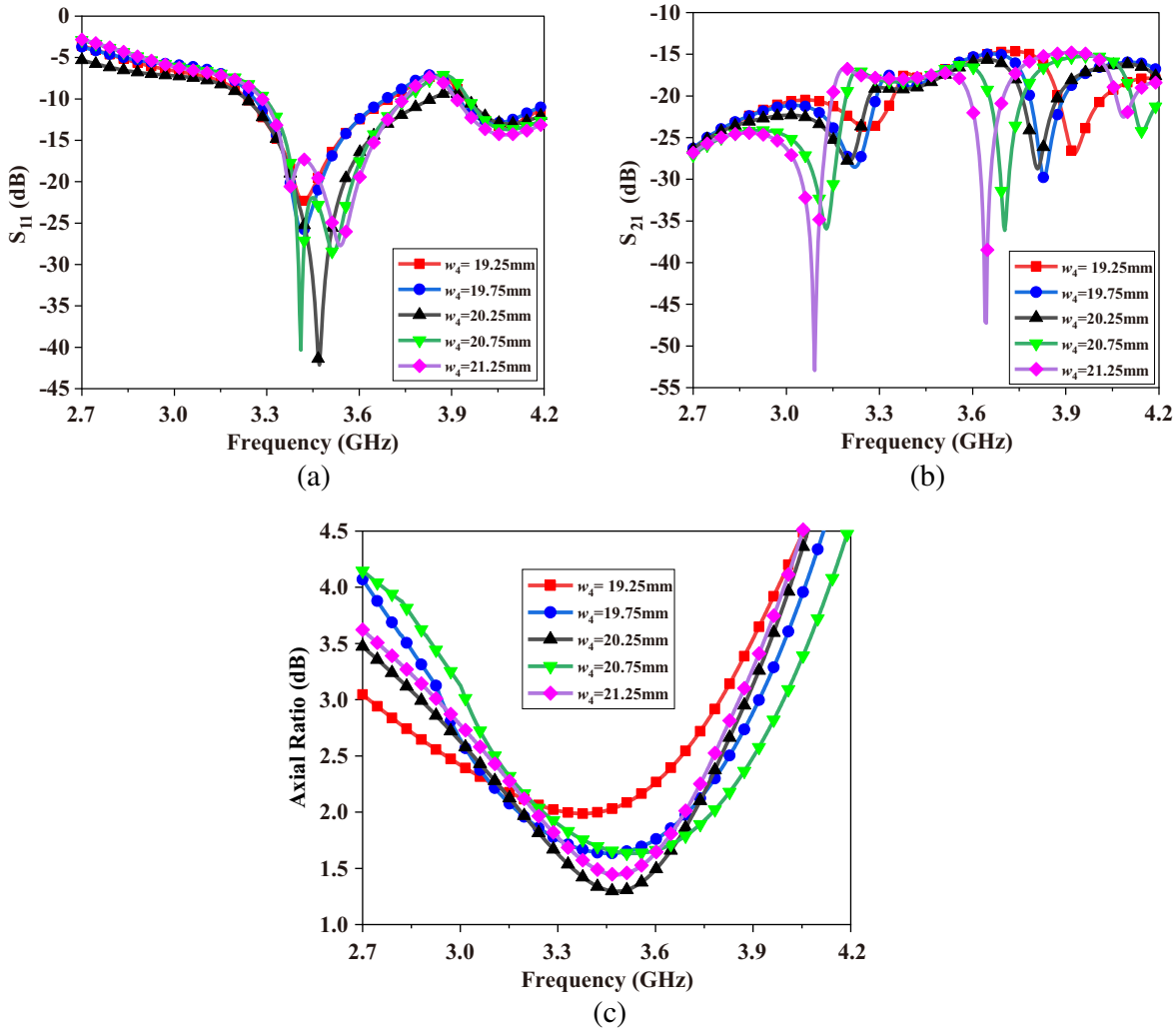

Figure 11. Variation of: (a) S_{11}; (b) S_{21}; (c) axial ratio with different length w_4.

2.2.3. Parametric Analysis

Figure 8 shows that the important parameters of the decoupling structure of MIMO antenna are the linear length (l_3) and the linear length (w_4). Therefore, the optimal size of the decoupling structure can be determined through the parameter analysis of l_3 and w_4. To study about the performance of the decoupling structure of the dual-CP MIMO antenna, a parametric analysis on the dimensions of the decoupling structure is performed as illustrated in Figures 10, 11. One of the design parameters is varied while the other parameters are kept constant to obtain the optimized size of the decoupling element of the MIMO antenna. The resonant frequency (S_{11}), isolated frequency (S_{21}), and ARBW of the proposed antenna can be enhanced by adjusting the linear length (l_3) of the I-shaped strip and the linear length (w_4) of the II-shaped strip in the decoupling element.

The S_{11}, S_{21} and axial ratio variations as a function of the linear length (l_3) of the I-shaped strip are shown in Figures 10(a), (b), (c), respectively. The S_{11} of the antenna shifts to higher sides with the increase of l_3, as shown in Figure 10(a). In addition, the second resonant frequency of the proposed antenna appears when l_3 increases to greater than 7 mm. Figure 10(b) shows that as the value of l_3 increases, the S_{21} of the decoupling component shifts to a lower frequency range, while the maximum isolation value basically does not change. Figure 10(c) shows that the axial ratio frequency of the antenna is greatly affected by the value of l_3. The increase in the value of l_3 causes the high-side offset of the center frequency and the reduction of the ARBW.

Similarly, the S_{11}, S_{21} and axial ratio variations as a function of the linear length (w_4) of the II-shaped strip are shown in Figures 11(a), (b), (c). The change trend of the S_{11} and S_{21} of the MIMO antenna due to the change of w_4 is basically the same as that of l_3. The increase in the value of w_4 causes S_{11} to move to high frequency and S_{21} to low frequency. Figure 11(c) shows that the impedance matching of the axial ratio of the MIMO antenna is optimal at $w_4 = 20.25\,\text{mm}$. Considering the above parameter analysis, the optimal size selection of the decoupling structure is as follows: $l_3 = 7\,\text{mm}$, $w_4 = 20.25\,\text{mm}$.

3. RESULTS AND DISCUSSION

The dual-CP MIMO antenna has been successfully simulated, fabricated, and measured. The proposed antenna prototype (top and bottom view) is presented in Figure 12(a). The total size of the presented antenna is $55 \times 55 \times 1.6\,\text{mm}^3$. SMA connectors are used for experimental measurements. The proposed dual-CP MIMO antenna prototype measurement setup inside the Satimo-SG64 anechoic chamber system is shown in Figure 12(b).

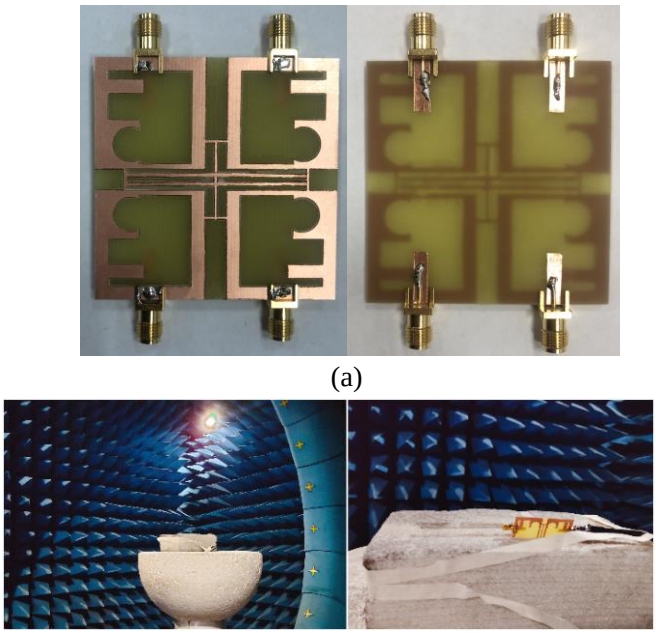

Figure 12. Proposed dual-CP MIMO antenna: (a) prototype; (b) measurement in anechoic chamber.

The S-parameters of the antenna were measured using an Agilent N5244A Vector Network Analyzer (VNA). The simulated and measured reflection coefficients of the proposed dual-CP MIMO antenna are shown in Figures 13(a), (b). The S-parameters (S_{11}, S_{22}, S_{33}, S_{44}) of all four ports are almost similar because the resonant components are the identical. Measurement results show that the proposed antenna worked in the frequency band of 3.28 to 3.80 GHz (520 MHz). Besides, the isolation value between different ports of the dual-CP MIMO antenna is greater than 16 dB in Figure 13(c). In the measurement, one antenna port is excited while other ports are matched with the 50 Ω loads.

It is observed from Figure 14 that a good quality of circular polarization (3.28–3.80 GHz) is achieved in the band of interest. The use of I-shaped and II-shaped strips between the ground planes improves the isolation between the antenna elements while maintaining the ARBW (2.85–3.87 GHz) of the antenna. The measured gain ranges from 3.4 to 5.3 dBi in the resonating range (3.28–3.80 GHz) of the antenna.

The diversity performance of the MIMO antenna is evaluated by measuring the envelope correlation coefficient (ECC) between the four ports. For a multi-antenna system, the ECC is expressed as

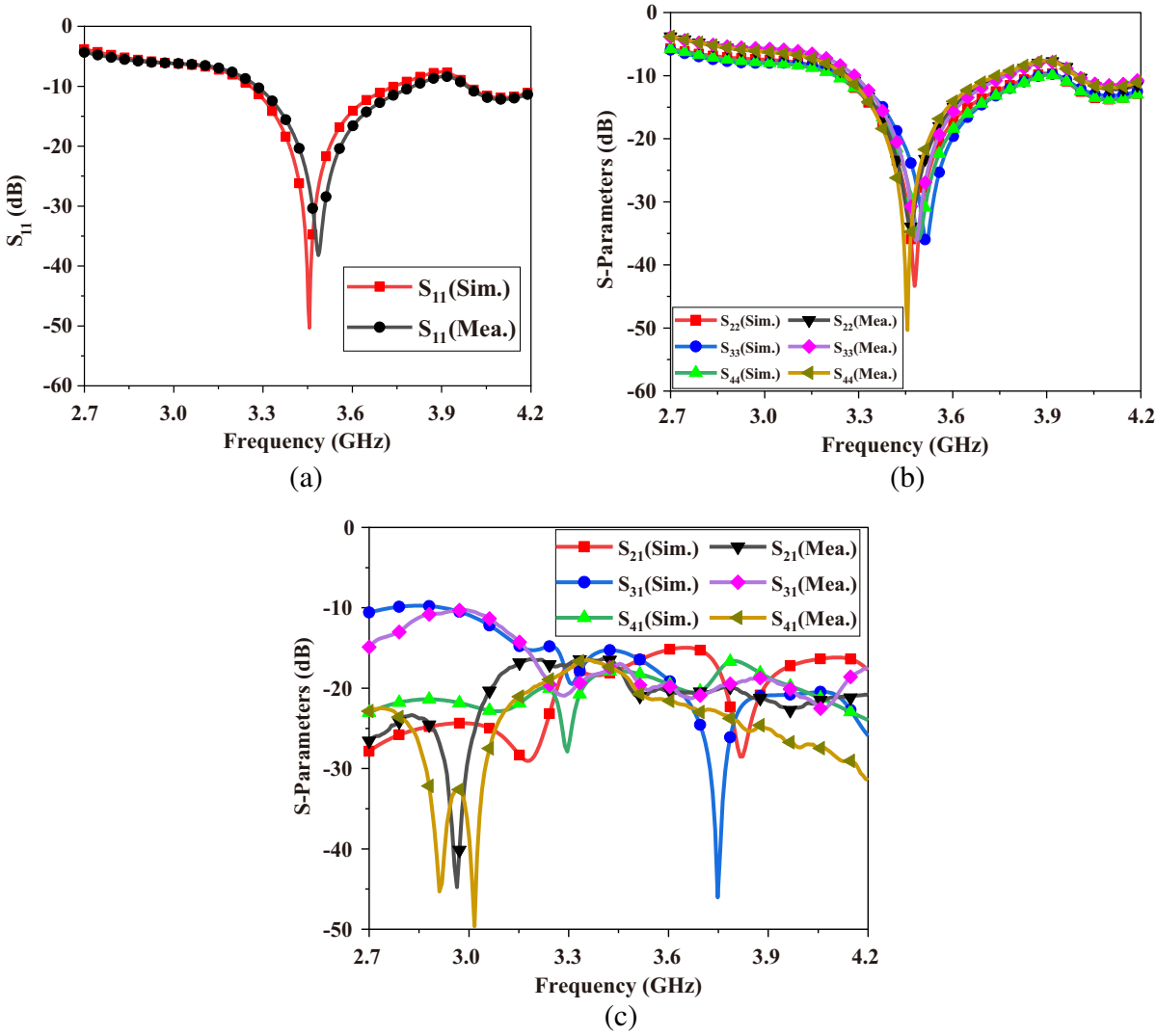

Figure 13. S-parameters (simulated and measured) result of the proposed dual-CP MIMO antenna at (a) S_{11}; (b) reflection coefficients; (c) S_{21}, S_{31}, S_{41}.

Eq. (1) [18]:

$$\rho_e = \frac{\left|S_{11}^* S_{12} + S_{12}^* S_{22} + S_{13}^* S_{32} + S_{14}^* S_{42}\right|}{\left(1 - |S_{11}|^2 - |S_{21}|^2 - |S_{31}|^2 - |S_{41}|^2\right)\left(1 - |S_{12}|^2 - |S_{22}|^2 - |S_{32}|^2 - |S_{42}|^2\right)} \quad (1)$$

Figure 15 shows that the ECC is less than 0.07 between various antenna ports, which verifies the diversity performance of the proposed dual-CP MIMO antenna.

The simulated and measured radiation patterns of the proposed dual-CP-MIMO antenna at 3.45 GHz are shown in Figure 16. The antenna emits LHCP waves when port-1/port-4 is excited and RHCP waves when port-2/port-3 is excited, showing dual-CP characteristics.

Table 2 compares the performance of the proposed dual-CP-MIMO antenna with some related works already reported. It can be observed that the proposed antenna could achieve good antenna performance for compact element separation distance. The proposed antenna contains four ports in a compact size and covers the lower frequency band (3.28 GHz–3.80 GHz), compared with the reported two-port dual-CP antenna [3, 15, 16]. The decoupling element of the antenna composed of I-shaped and II-shaped metal strips can optimize isolation and ARBW. The proposed antenna has a wide ARBW which is 30.3% (2.85–3.87 GHz). The ARBW of the reported MIMO antenna is 1.5% (5.744–5.830 GHz) [11].

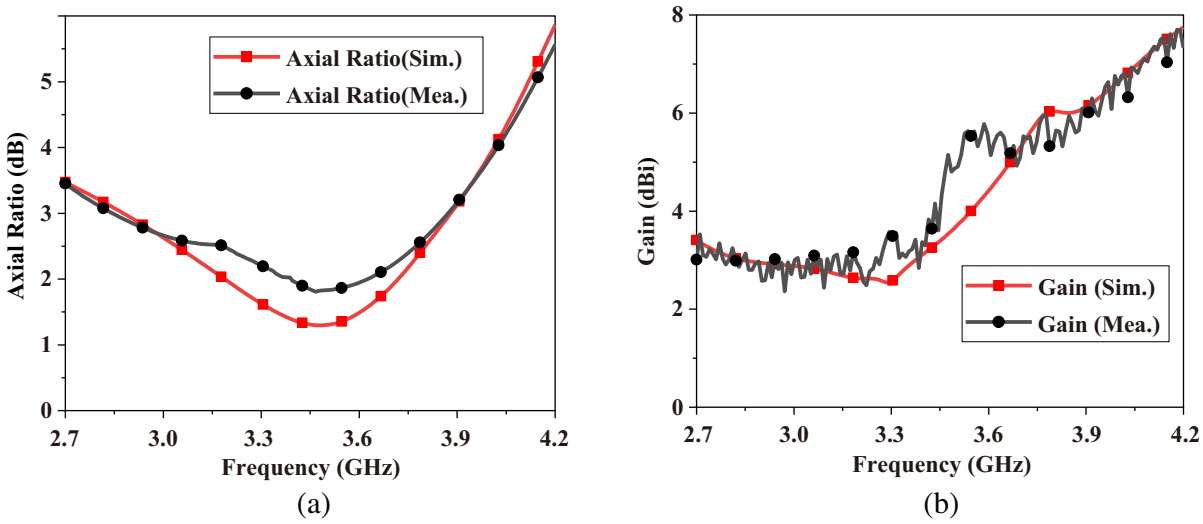

Figure 14. Simulated and measured of the proposed dual-CP MIMO antenna: (a) axial ratio; (b) gain.

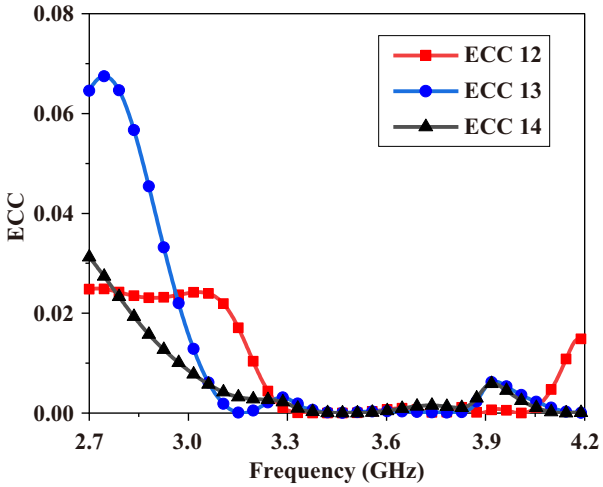

Figure 15. ECC of the proposed dual-CP MIMO antenna.

Table 2. Comparison of the proposed dual-CP MIMO antenna with other MIMO antennas.

Ref	No. of Ports	Size (mm^3)	Impedance Bandwidth (GHz)	3-dB ARBW (GHz)	ECC	Isolation (dB)	Peak Gain (dBi)	Connected Ground
[3]	2	23×29	8.07–11.59	8.11–10.56	0.05	> 20	4	Yes
[15]	2	$13.7 \times 36.2 \times 0.813$	5.2–6.3	5.2–6.3	0.002	> 22	5.8	No
[16]	2	$100 \times 150 \times 0.8$	2.47–2.55	2.5–2.66	0.003	> 20	6.1	Yes
[11]	4	$27.69 \times 97 \times 1.524$	5.49–6.024	5.744–5.83	0.15	> 33	5.34	No
[19]	4	$60 \times 60 \times 1.6$	3.4–3.8	3.46–3.7	0.12	> 19	4.5	Yes
[20]	4	$70 \times 68 \times 1.6$	4–13	4.2–8.5	0.25	> 18	6.4	Yes
Prop.	4	$55 \times 55 \times 1.6$	3.28–3.80	2.88–3.88	0.07	> 16	5.3	Yes

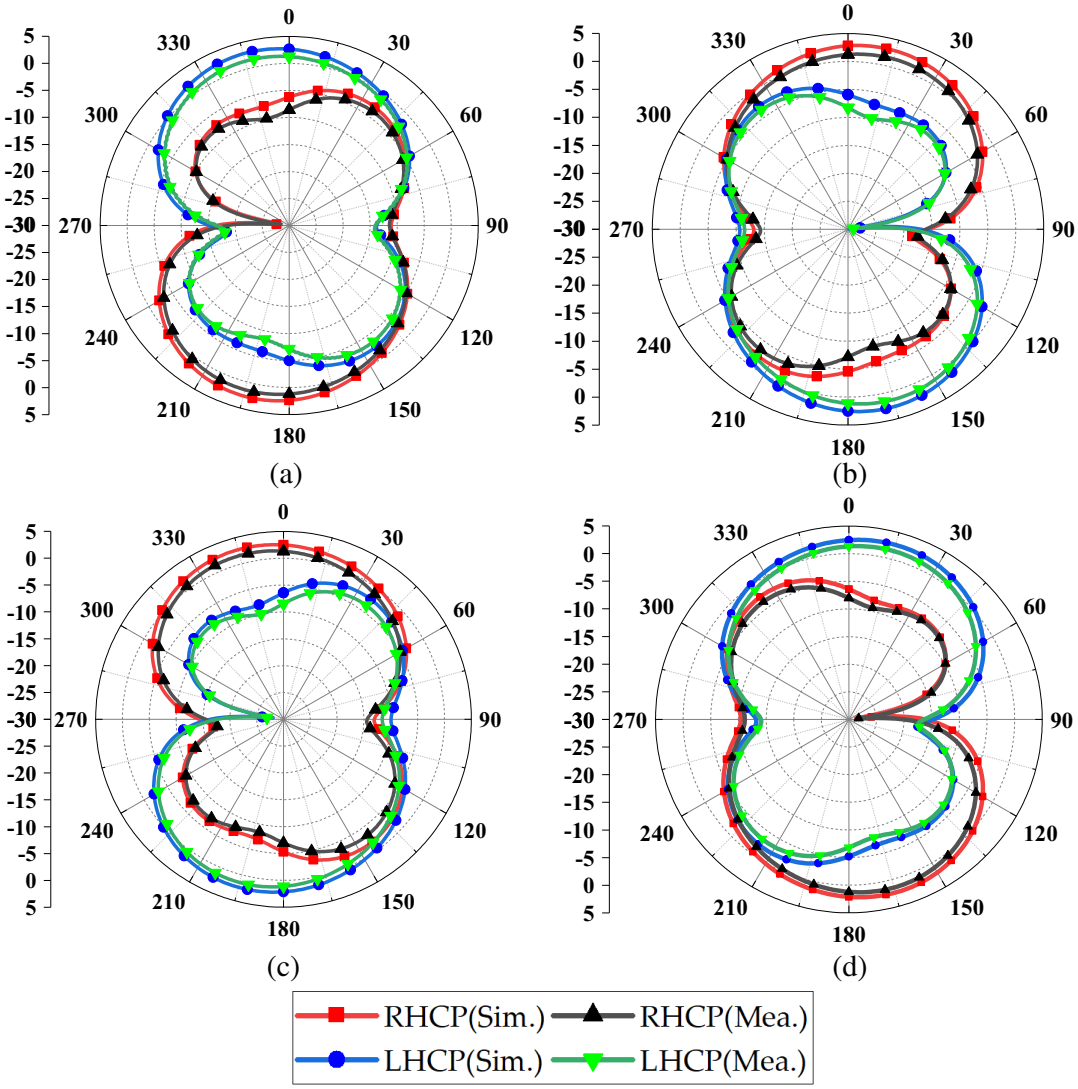

Figure 16. Radiation patterns at 3.45 GHz when (a) port-1 is excited; (b) port-2 is excited; (c) port-3 is excited; (d) port-4 is excited.

Compared with the reported four-port dual-CP antenna [19, 20], the proposed antenna achieves full coverage of CP characteristics in the frequency band of interest. Besides, the antennas [11, 15] cannot be used in practical application because of the disconnection of ground plane. The above comparison shows the excellent performance of the dual CP-MIMO antenna with connected ground proposed in this paper. Changing the linear length (l_3 and w_4) of the decoupling element to adjust the resonant frequency of the antenna can make it adapt to different application requirements. The proposed antenna is suitable for Sub-6G (NR band number: n78) band applications.

In particular, the reported antenna produces the LHCP wave through the ground plane with the circular stub and the offset feed line position [4]. The proposed antenna radiates dual-CP waves by arranging the circularly polarized antenna element and its mirror image on a square substrate. The feed location of the reported antenna element is shifted towards the right side to obtain a lower frequency band and adopts the structure of an open hexagonal slot on the ground to achieve CP characteristics. Besides, the inter-element spacing is $0.12\lambda_0$ (for $f_c = 3.6$ GHz) between the MIMO radiating elements [19]. The feed location of the proposed antenna element is in the middle, and it adopts the structure of double rectangular strips on the same side to achieve CP characteristics. The

inter-element spacing is $0.057\lambda_0$ (for $f_c = 3.45\,\text{GHz}$) between MIMO radiating elements to maintain the 3-dB ARBW of the antenna element. The reported antenna realizes circular polarization characteristics through a G-shaped radiating element. An arc-shaped region is etched out from the rectangular ground plane beneath the radiator to improve impedance matching [20]. The low-frequency operating frequency of the proposed antenna is achieved by etching a semi-circular slot in the rectangular strip. Among these CP MIMO antennas reported above, the proposed dual-CP MIMO antenna achieves good isolation and wide axis ratio bandwidth in a more compact structure.

4. CONCLUSION

A compact microstrip four-port dual-CP MIMO antenna is proposed and analysed. The antenna is composed of four identical microstrip line feeder antenna elements and its mirror image, and the circular polarization characteristics are achieved by rectangular strips in the same direction. The proposed MIMO antenna radiates LHCP waves when radiators 1 and 4 are excited and radiates RHCP waves when radiators 2 and 3 are excited. According to the measurement results of the antenna, the ARBW of the antenna is 2.85–3.87 GHz (30.3%), which completely covers the impedance bandwidth of 3.28–3.80 GHz (14.6%). The ECC and isolation of the MIMO antenna are at an acceptable level. The proposed antenna can be used in practical applications because of its common ground plane. Accordingly, the proposed antenna is propitious to Sub-6G band applications. At the same time, it is suitable for dual-CP communication systems and polarization diversity systems.

REFERENCES

1. Dicandia, F. A., S. Genovesi, and A. Monorchio, "Analysis of the performance enhancement of MIMO systems employing circular polarization," *IEEE Transactions on Antennas and Propagation*, Vol. 65, No. 9, 4824–4835, 2017.
2. Saxena, S., B. K. Kanaujia, S. Dwari, S. Kumar, and R. Tiwari, "Compact microstrip antennas with very wide ARBW and triple circularly polarized bands," *International Journal of RF and Microwave Computer-Aided Engineering*, Vol. 28, No. 1, 2018.
3. Kumar, S., K. W. Kim, H. C. Choi, R. Tiwari, M. K. Khandekwal, S. K. Palaniswamy, and B. K. Kanaujia, "A low profile circularly polarized UWB antenna with integrated GSM band for wireless communication," *AEU-International Journal of Electronics and Communications*, Vol. 93, 224–232, 2018.
4. Kumar, S., G. H. Lee, D. H. Kim, W. Mohyuddin, H. C. Choi, and K. W. Kim, "A compact four-port UWB MIMO antenna with connected ground and wide axial ratio bandwidth," *International Journal of Microwave and Wireless Technologies*, Vol. 12, No. 1, 75–85, 2019.
5. Malik, J., A. Patnaik, and M. V. Kartikeyan, "Novel printed MIMO antenna with pattern and polarization diversity," *IEEE Antennas and Wireless Propagation Letters*, Vol. 14, 739–742, 2015.
6. Sharma, Y., D. Darkar, K. Saurav, and K. V. Srivastava, "Three-element MIMO antenna system with pattern and polarization diversity for WLAN applications," *IEEE Antennas and Wireless Propagation Letters*, Vol. 16, 1163–1166, 2017.
7. Akbari, M., H. A. Ghalyon, M. Farahni, A.-R. Sebak, and T. A. Denidni, "Spatially decoupling of CP antennas based on FSS for 30-GHz MIMO systems," *IEEE Access*, Vol. 5, 6527–6537, 2017.
8. Parbat, R. S., A. R. Tambe, M. B. Kadu, and R. P. Labade, "Dual polarized triple band 4×4 MIMO antenna with novel mutual coupling reduction approach," *2015 IEEE Bombay Section Symposium (IBSS)*, 2015.
9. Saxena, S., B. K. Kanaujia, S. Awari, S. Kumar, and R. Tiwari, "A compact dual-polarized MIMO antenna with distinct diversity performance for UWB applications," *IEEE Antennas and Wireless Propagation Letters*, Vol. 16, 3096–3099, 2017.
10. Saurav, K., N. K. Mallat, and Y. M. M. Antar, "A three-port polarization and pattern diversity ring antenna," *IEEE Antennas and Wireless Propagation Letters*, Vol. 17, No. 7, 1324–1328, 2018.

11. Malviya, L., R. K. Panigrahi, and M. Kartikeyan, "Circularly polarized 2×2 MIMO antenna for WLAN applications," *Progress In Electromagnetics Research C*, Vol. 66, 97–107, 2016.
12. Jalali, M., M. Naser-Moghadasi, and R. A. Sadeghzadeh, "Dual circularly polarized multilayer MIMO antenna array with an enhanced SR-feeding network for C-band application," *International Journal of Microwave and Wireless Technologies*, Vol. 9, No. 8, 1741–1748, 2017.
13. Sahli, R. K. and S. Dwari, "A broadband dual circularly polarized square slot antenna," *IEEE Transactions on Antennas and Propagation*, Vol. 64, No. 1, 290–294, 2016.
14. Li, Z., X. Zhu, and C. Yin, "CPW-fed ultra-wideband slot antenna with broadband dual circular polarization," *AEU-International Journal of Electronics and Communications*, Vol. 98, 191–198, 2019.
15. Ullah, U., I. B. Mabrouk, and S. Koziel, "Enhanced-performance circularly polarized MIMO antenna with polarization/pattern diversity," *IEEE Access*, Vol. 8, 11887–11895, 2020.
16. Jamal, M. Y., M. Li, and K. L. Yeung, "Isolation enhancement of closely packed dual circularly polarized MIMO antenna using hybrid technique," *IEEE Access*, Vol. 8, 11241–11247, 2020.
17. Sharawi, M. S., "Current misuses and future prospects for printed multiple-input, multiple-output antenna systems," *IEEE Antennas and Propagation Magazine*, Vol. 59, No. 2, 162–170, 2017.
18. Blanch, S., J. Romeu, and I. Corbella, "Exact representation of antenna system diversity performance from input parameter description," *Electronics Letters*, Vol. 39, No. 9, 705–707, 2003.
19. Saxena, S., B. K. Kanaujia, S. Dwari, S. Kumar, H. C. Choi, and K. W. Kim, "Planar four-port dual circularly-polarized MIMO antenna for sub-6 GHz band," *IEEE Access*, Vol. 8, 90779–90791, 2020.
20. Kumar, S., G. H. Lee, D. H. Kim, H. C. Choi, and K. W. Kim, "Dual circularly polarized planar four-port MIMO antenna with wide axial-ratio bandwidth," *Sensors (Basel)*, Vol. 20, No. 19, 2020.